Two trapped particles interacting by a finite-range two-body potential in two spatial dimensions

Rostislav A. Doganov,[1] Shachar Klaiman,[1] Ofir E. Alon,[2] Alexej I. Streltsov,[1] and Lorenz S. Cederbaum[1]
[1]*Theoretische Chemie, Physikalisch-Chemisches Institut, Universität Heidelberg, Im Neuenheimer Feld 229, D-69120 Heidelberg, Germany*
[2]*Department of Physics, University of Haifa at Oranim, Tivon 36006, Israel*
(Received 24 October 2012; published 28 March 2013)

We examine the problem of two particles confined in an isotropic harmonic trap, which interact via a finite-range Gaussian-shaped potential in two spatial dimensions. We derive an approximative transcendental equation for the energy and study the resulting spectrum as a function of the interparticle interaction strength. Both the attractive and repulsive systems are analyzed. We study the impact of the potential's range on the ground-state energy. We also explicitly verify by a variational treatment that in the zero-range limit the positive δ potential in two dimensions only reproduces the noninteracting results, if the Hilbert space in not truncated, and demonstrate that an extremely large Hilbert space is required to approach the ground state when one is to tackle the limit of zero-range interaction numerically. Finally, we establish and discuss the connection between our finite-range treatment and regularized zero-range results from the literature. The present results indicate that a finite-range interparticle potential is numerically amenable for treating the statics and the nonequilibrium dynamics of interacting many-particle systems (bosons) in two dimensions.

DOI: 10.1103/PhysRevA.87.033631 PACS number(s): 03.75.Hh, 34.20.−b, 03.65.−w

I. INTRODUCTION

In recent years there has been an increasing interest in two-dimensional (2D) quantum systems. The condensed-matter community has long been investigating 2D quantum effects, for example, in relation to superfluid films [1,2], high-temperature superconductivity [3–5], and low-dimensional materials, such as graphene [6,7] and quantum dots, see, e.g., [8]. The rapid progress in atomic trapping and cooling now also allows one to study quantum systems with reduced dimensionality in the context of ultracold trapped gases [9]. Degenerate quasi-2D Bose and Fermi gases have already been produced in highly anisotropic "pancake" traps [10–15]. This opens up the unique possibility to investigate the rich palette of 2D quantum effects and phases in a highly controlled environment.

In dilute systems, such as the ultracold trapped gases, interactions are usually described by a two-particle zero-range effective potential. This approach has been particularly fruitful in one dimension, where the δ function interaction is well behaved and there is a simple relation between the scattering length and the interaction parameter. In two and three dimensions, however, the δ function is not a self-adjoint operator [16,17], which gives rise to various anomalies [16,18–22]. In particular, there is no scattering from a positive 2D δ function and, for a negative one, the bound-state energy diverges. Several approaches to overcome the arising problems and to model zero-range interactions in 2D have been proposed in the literature: self-adjoint extensions [23,24], renormalization techniques [18–20], regularization of the δ potential [17,25,26], modified boundary conditions [27,28], and a coupled-channel model [29].

The analytically tractable problem of two harmonically trapped particles interacting via a zero-range potential in 2D has previously been addressed using a regularized δ function [17,26] and Bethe-Peierls boundary conditions [28]. These works have obtained and studied the spectrum of the particles with zero-range interaction as a function of the 2D scattering length [17,28]. In the limit of zero-range interaction, it has been shown that the results are universal, i.e., the spectrum is independent of the details of short-range potential; see [26]. Recently in [30], finite-range corrections to the Busch model [17] in 2D using a Green's function approach have been derived.

In the present work we are interested in the physics of a truly *finite-range* potential, and examine the problem of two harmonically trapped particles in 2D interacting via a finite-range two-body potential modeled by a Gaussian function. We derive an approximative, yet accurate, transcendental equation for the energy, and present the resulting spectrum. In particular, we study the energy levels for both positive and negative interaction and explore the role of the *range* of the potential on the ground-state energy. Furthermore, we demonstrate that an extremely large Hilbert space is required to approach the ground state when one is to tackle the limit of zero-range interaction numerically. Last but not least, we establish and discuss the connection between our finite-range results and previous zero-range works.

We recall that, in one dimension, the use of the common δ-function interaction is well established and easy to handle. Unfortunately, in 2D as mentioned above, the 2D δ interaction cannot be used analogously to its one-dimensional counterpart. Whereas a regularized 2D contact potential is analytically tractable, it is harder to work with numerically. Furthermore, for more than two particles, analytical treatments quickly become inaccessible, leaving one only with a numerical recourse. For the numerical many-body simulations one usually prefers and it is often only practical to use smooth, finite-range, model interaction potentials.

In Ref. [31], the Lee-Suzuki transformation is used to compute ground- and excited-state energies of up to 20 harmonically trapped bosons interacting by a Gaussian-shaped interaction in 2D. In our work we focus on the two-boson problem and explicitly show that a Gaussian-shaped two-body potential and its zero-range pseudopotential give similar results for both repulsive and attractive interactions except for the lowest eigenstate of the latter potential. For repulsive interaction the zero-range pseudopotential leads to an additional dimer bound state which is not connected to the unperturbed

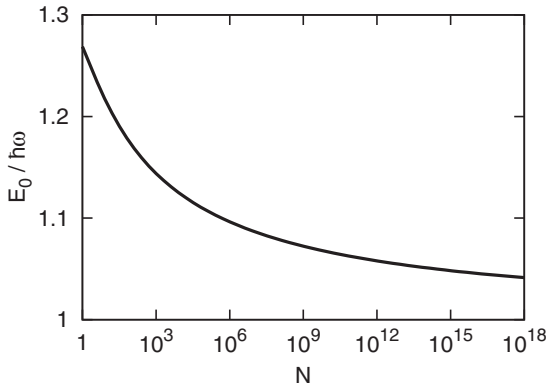

FIG. 1. Ground-state energy (in the center of mass frame) of two particles in a harmonic trap interacting via a (nonregularized) δ potential in 2D as a function of the size of the Hilbert space. The results are obtained by numerically solving Eq. (11) with $\lambda_0 = 1$, $l = 1$ and different N. Notice the logarithmic scale on the x axis. All quantities are dimensionless.

system when the interaction is switched off. Thus we can work with a Gaussian-shaped interaction in 2D, since this bound state is energetically strongly separated and will be difficult to reach in dynamics in general. In this context, the purpose of the present study is to lay down an analytical ground and computational rationale (see, e.g., Fig. 1 and related discussion below) to using a Gaussian-shaped interaction in modeling the statics, see for example [31], as well as the nonequilibrium dynamics of many trapped interacting bosons in 2D. There is much interest in the statics and the nonequilibrium dynamics of 2D Bose systems; see, e.g., [32,33]. We mention that, in one dimension, the usage of a finite-range interparticle interaction of a Gaussian shape has been shown to be justified and led to ample results on the statics and the nonequilibrium dynamics of a few trapped interacting bosons [34–42].

The article is organized as follows. In Sec. II we derive the general secular equation for the energy of two trapped particles interacting via the Gaussian-shaped two-body potential in 2D. In Sec. III, by utilizing a variational treatment, we briefly discuss the limit of a positive nonregularized δ potential and show that the energy spectrum of the noninteracting system is altered only as a consequence of truncating the Hilbert space. In Sec. IV A we present an efficient high-performance approximation for the finite-range interaction, and derive an equation for the energy of the two particles. Then, in Sec. IV B, we study the resulting energy spectrum and, in Sec. V, compare our finite-range findings to zero-range results from the literature. Finally, in Sec. VI, we summarize our results. Supplemental derivations and numerics are deferred to the Appendixes.

II. EIGENVALUE EQUATION

We consider two particles in an isotropic harmonic trap, which are interacting via a normalized two-body Gaussian-shaped potential. The Hamiltonian of the system is

$$H = \sum_{i=1}^{2}\left(-\frac{\hbar^2}{2m}\nabla_i^2 + \frac{1}{2}m\omega^2\bar{r}_i^2\right) + \lambda_0 V(\bar{r}_1 - \bar{r}_2), \quad (1)$$

$$V(\bar{r}_1 - \bar{r}_2) = \frac{1}{\pi s^2}e^{-\frac{(\bar{r}_1-\bar{r}_2)^2}{s^2}}. \quad (2)$$

Here ∇ is the 2D Nabla operator and $\bar{r} = (x, y)$. The problem can be separated into a noninteracting center of mass and an interacting relative part. With the standard definitions of a reduced mass, $\mu = m/2$, and a total mass, $M = 2m$, as well as center-of-mass and relative coordinates $\bar{R} = \frac{1}{2}(\bar{r}_1 + \bar{r}_2)$ and $\bar{r} = \bar{r}_1 - \bar{r}_2$, the Hamiltonian can be rewritten as $H = H_{\text{c.m.}} + H_{\text{rel}}$ with

$$H_{\text{c.m.}} = -\frac{\hbar^2}{2M}\nabla_R^2 + \frac{1}{2}M\omega^2 R^2, \quad (3)$$

$$H_{\text{rel}} = -\frac{\hbar^2}{2\mu}\nabla_r^2 + \frac{1}{2}\mu\omega^2 r^2 + \lambda_0 V(r). \quad (4)$$

Here $H_{\text{c.m.}}$ is the Hamiltonian of the 2D quantum harmonic oscillator whose solutions are well known. From now on we concentrate on the relative part, which we further write as $H_{\text{rel}} = H_0 + \lambda_0 V(r)$, where H_0 reads

$$H_0 = -\frac{\hbar^2}{2\mu}\nabla_r^2 + \frac{1}{2}\mu\omega^2 r^2. \quad (5)$$

We start by constructing a solution Ψ of the time-independent Schrödinger equation from the eigenstates of H_0. We take only eigenstates with zero angular momentum, which we denote $\varphi_k(r)$. The respective energies are $\varepsilon_k = (2k+1)\hbar\omega$. We note that all states with nonzero angular momentum vanish at the origin and, therefore, should not be significantly perturbed by the Gaussian potential if its width is sufficiently small. After substituting the expansion $\Psi = \sum_{i=0}^{\infty} c_k\varphi_k$ into the Schrödinger equation $H_{\text{rel}}\Psi = E\Psi$, and after projecting onto a state $\varphi_{k'}(r)$, we arrive at the secular equation:

$$c_{k'}(\varepsilon_{k'} - E) + \lambda_0\sum_{k=0}^{\infty} c_k\int \varphi_{k'}^*(r)V(r)\varphi_k(r)d\bar{r} = 0. \quad (6)$$

The integration is taken over the whole 2D plane with $d\bar{r} = 2\pi r\,dr$. To proceed further we need to evaluate the matrix elements appearing in the above sum. As we show in Appendix A, this can be done analytically. The result of the calculation is

$$I_{k',k}(s) = \int \varphi_{k'}^*(r)V(r)\varphi_k(r)d\bar{r} = \frac{1}{\pi l^2}\left(\frac{1}{\left(\frac{s}{l}\right)^2+1}\right)^{k'+k+1} {}_2F_1\left(-k', -k; 1, \left(\frac{s}{l}\right)^4\right). \quad (7)$$

Here, ${}_2F_1$ is the Gauss hypergeometric function [43] and $l = \sqrt{\frac{\hbar}{\mu\omega}}$ is the harmonic-oscillator length.

III. SOLUTION FOR CONTACT POTENTIAL

Before proceeding to the results for a finite-range interaction, let us first examine the limit $s \to 0$, in which case the normalized Gaussian-shaped potential defined in Eq. (2) goes into a δ function. For $s = 0$ Eq. (7) takes on the form $I_{k',k}(0) = \frac{1}{\pi l^2}$ and the matrix elements are independent of the indices k' and k. In this limit Eq. (6) reduces to

$$c_{k'}(\varepsilon_{k'} - E) + \lambda_0\sum_{k=0}^{\infty}\frac{1}{\pi l^2}c_k = 0. \quad (8)$$

The sum appearing in the above equation runs over all indices k. After rearranging the expansion coefficients, we obtain

$$c_{k'} = \frac{-\lambda_0 C}{\varepsilon_{k'} - E}, \tag{9}$$

where C is a parameter which can depend on the energy E, but is the same for all k'. By substituting the above expression for the coefficients c_k back into Eq. (8) and multiplying by $\pi l^2/\lambda_0$, we arrive at

$$\frac{\hbar\omega\pi l^2}{\lambda_0} + \sum_{k=0}^{\infty} \frac{1}{2k+1-E/\hbar\omega} = 0. \tag{10}$$

The sum in the above equation is a general harmonic series and is divergent [44]. The anomaly associated with a contact potential in 2D stems from this diverging sum in the current treatment. To obtain a meaningful expression we first truncate the sum at finite N and then examine the behavior for $N \to \infty$:

$$\frac{\hbar\omega\pi l^2}{\lambda_0} + \sum_{k=0}^{N} \frac{1}{2k+1-E/\hbar\omega} = 0. \tag{11}$$

From the above equation we can determine the energy spectrum of the two trapped particles interacting via a δ potential in 2D for a given truncation N.

Let us consider the solution of Eq. (11) closest to one of the poles appearing in the equation, say, the pole specified by $k = k'$. We may write $E/\hbar\omega = 2k' + 1 + \Delta k'$. This immediately leads to

$$\frac{1}{\Delta k'} = \frac{\hbar\omega\pi l^2}{\lambda_0} + \sum_{k\neq k'}^{N} \frac{1}{2k+1-E/\hbar\omega}. \tag{12}$$

For large N the sum on the right-hand side (RHS) grows logarithmically with N for any value of $E \neq 2k+1$ ($k \neq k'$), and hence $\Delta k'$ approaches zero as $\sim 1/\ln N$. Thus, by increasing N, we can make the energy levels arbitrarily close to the eigenvalues of the respective noninteracting system. These considerations explicitly show that in 2D the positive (nonregularized) δ potential modifies the spectrum of two trapped particles only as a consequence of restricting the Hilbert space. We point out that the noninteracting values are approached logarithmically because the series in Eq. (11) diverges logarithmically. We illustrate this in Fig. 1, where we plot the energy of the lowest state obtained from Eq. (11) for increasing N. We stress that the above considerations are rigorous and Eq. (11) can be viewed as a variational ansatz (see Appendix B).

IV. FINITE-RANGE POTENTIAL

A. Efficient high-performance approximation

In order to obtain an (approximative) equation for the energy of the two particles in the finite-range case, $s > 0$, we proceed analogously to the treatment above and make an ansatz for the expansion coefficients $c_{k'}$. To this end we use an ansatz similar, but not identical, to the one obtained in the Brillouin-Wigner perturbation theory (see discussion in Appendix C),

$$c_k = \frac{-\lambda_0 I_{0,k}(s)}{\varepsilon_k - E} C, \tag{13}$$

and obtain an equation for E by substituting this expression into Eq. (6). Since we have $I_{0,k}(0) = \frac{1}{\pi l^2} = \text{const}$, this ansatz ensures that for $s \to 0$ we exactly recover the δ potential limit of Eq. (9), which was discussed in the previous section. We stress that the current approximation in not variational, in contrast to the case $s = 0$. However, we establish the high accuracy of the treatment by comparing to full direct diagonalization and zero-range results (see Appendix D and Sec. V).

By substituting (13) into Eq. (6) and rearranging terms, we obtain

$$\frac{\hbar\omega}{\lambda_0} I_{0,k'} + \sum_{k=0}^{\infty} \frac{I_{0,k}(s) I_{k',k}(s)}{\varepsilon_k/\hbar\omega - E/\hbar\omega} = 0. \tag{14}$$

For each index value k' the above expression gives an equation for E. By setting $k' = 0$ the matrix elements $I_{k',k}(s)$ take on the form $I_{0,k} = \frac{1}{\pi l^2}\left(\frac{1}{(\frac{s}{l})^2+1}\right)^{k+1}$ and the equation for E becomes

$$\frac{\hbar\omega}{\lambda_0} I_{0,0} + \sum_{k=0}^{\infty} \frac{I_{0,k}^2(s)}{\varepsilon_k/\hbar\omega - E/\hbar\omega} = 0. \tag{15}$$

The series $\sum_{k=0}^{\infty} \frac{I_{0,k}^2}{\varepsilon_k/\hbar\omega - E/\hbar\omega}$ can be expressed in terms of the Lerch transcendent function $\Phi(z,s,\alpha)$ [45]

$$\begin{aligned} &\sum_{k=0}^{\infty} \frac{I_{0,k} I_{k,0}}{\varepsilon_k/\hbar\omega - E_m/\hbar\omega} \\ &= \frac{1}{(\pi l^2)^2} \sum_{k=0}^{\infty} \frac{1}{2k+1-E/\hbar\omega} \left(\frac{1}{\left(\frac{s}{l}\right)^2+1}\right)^{2(k+1)} \\ &= \frac{\Phi\left(\frac{1}{[1+(s/l)^2]^2}, 1, \frac{1-E/\hbar\omega}{2}\right)}{2\pi^2 l^4 [1+(s/l)^2]^2}. \end{aligned} \tag{16}$$

The final equation for the energy of the two trapped particles in the center-of-mass frame reads

$$-\frac{\Phi\left(\frac{1}{[1+(s/l)^2]^2}, 1, \frac{1-E/\hbar\omega}{2}\right)}{2\pi l^2 [1+(s/l)^2]} = \frac{\hbar\omega}{\lambda_0}. \tag{17}$$

Equation (17) is the main analytical result of the paper. It allows one to obtain the energy spectrum of two trapped particles interacting via a Gaussian-shaped potential in 2D for given parameters λ_0, s, and l.

B. Energy spectrum

In this section we present the energy spectrum (in the center-of-mass frame) of two trapped particles interacting via a Gaussian-shaped potential in 2D, which results from Eq. (17). From now on we fix the harmonic-oscillator length to $l = 1$. We first set $s/l = 0.1$ and explore the dependence of the energy levels on the parameter λ_0. The energies of the first three states versus λ_0 are plotted in Fig. 2. For $\lambda_0 > 0$ the energies are always above the respective noninteracting values and the system is repulsive. As expected, at $\lambda_0 \to 0$ we recover the noninteracting values $E/\hbar\omega = 2k+1$, which correspond to the poles of the left-hand side (LHS) of Eq. (17). For $\lambda_0 < 0$ the particles are interacting attractively and the ground-state energy quickly diverges to $-\infty$ for $\lambda_0 \to -\infty$.

The Gaussian-shaped two-body potential also allows us to study the role of the range, s, of the interaction. In Fig. 3 we

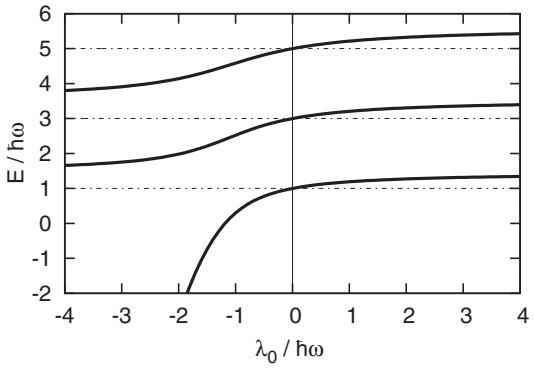

FIG. 2. Energies of the first three states (in the center-of-mass frame) of two trapped particles in 2D interacting via a Gaussian-shaped potential versus the interaction strength λ_0. The dashed-dotted lines show the energies of the respective noninteracting system. Here $l = 1$ and $s/l = 0.1$. All quantities are dimensionless.

show the dependence of the ground-state energy on s for three different values of the parameter λ_0. For repulsive interactions, i.e., $\lambda_0 > 0$, we find that with decreasing s the ground-state energy logarithmically approaches the noninteracting value $\hbar\omega$. This is in agreement with our discussion of the 2D δ potential in Sec. III. We note that this behavior is also in agreement with the formal result in [46], where it is proven that in two and more dimensions the solutions of the Schrödinger equation are not affected by positive potentials with vanishing support. For attractive interactions ($\lambda_0 < 0$) the dependence on s is more pronounced and we observe that in the limit $s \to 0$ the energy of the ground state diverges to $-\infty$ for any negative λ_0. This result is also consistent with previous studies, where it was observed that the attractive (nonregularized) δ potential yields a bound state with an infinitely negative energy. This is, in fact, the starting point for renormalization treatments [20,47].

V. COMPARISON WITH ZERO-RANGE RESULTS

The energy spectrum of two harmonically trapped particles with a zero-range interaction in 2D has previously been

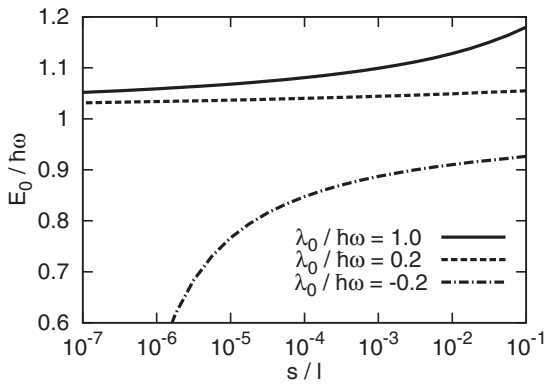

FIG. 3. Energy of the ground state (in the center-of-mass frame) of two trapped particles in 2D interacting via a Gaussian-shaped potential versus the width of the interaction, s, for different choices of $\lambda_0/\hbar\omega$. See legend inside the graph. Notice the logarithmic scale on the x axis. All quantities are dimensionless.

obtained in the literature using a regularized δ potential [17], general scattering arguments [26], and modified boundary conditions [28]. In all three works, the authors derive a transcendental equation for the energy, which can be written in the form

$$\tilde{\psi}\left(\frac{1 - E/\hbar\omega}{2}\right) = \ln\left(\frac{l^2}{2a_{2D}^2}\right) + A. \tag{18}$$

Here $\tilde{\psi}(x)$ denotes the digamma function, a_{2D} is the 2D scattering length, and l is the harmonic-oscillator length. The interaction strength is controlled through an interaction parameter defined as $\ln(\frac{l^2}{2a_{2D}^2})^{-1}$ [17,26]. The constant factor A, which is slightly different within the works [17,26,28], depends on the exact form for the effective range expansion that the respective authors use (see the discussion at the end of [26]) and has no consequence on the following analysis.

In order to relate our finite-range result for the energy of two trapped interacting particles to the zero-range treatments, we employ a Taylor expansion of the LHS of Eq. (17) around $s = 0$ [48],

$$-\frac{\Phi\left(\frac{1}{[1+(s/l)^2]^2}, 1, \frac{1-E/\hbar\omega}{2}\right)}{2\pi l^2[1 + (s/l)^2]} \approx \frac{1}{2\pi l^2}\left[\tilde{\psi}\left(\frac{1 - E/\hbar\omega}{2}\right) + \ln\left(\frac{2s^2}{l^2}\right) + \gamma\right] + O[s]. \tag{19}$$

Here $\gamma \approx 0.577(2)$ is the Euler-Mascheroni constant and $\tilde{\psi}(x)$ is again the digamma function. By neglecting terms of order $O[s]$ and after rearranging, we can rewrite Eq. (17) for $s \approx 0$ as

$$\tilde{\psi}\left(\frac{1 - E/\hbar\omega}{2}\right) = \frac{2\pi l^2}{\lambda_0/\hbar\omega} + \tilde{A}(s), \tag{20}$$

with $\tilde{A}(s) = -\ln(\frac{2s^2}{l^2}) - \gamma$. Evidently, the above equation for the energy has the same form as the literature result in (18), and by an appropriate choice of λ_0 and s our ansatz reproduces the zero-range spectrum. By comparing the RHS of Eqs. (20) and (18), we immediately see that (for weak interactions) the interaction parameter is equal to $\frac{\lambda_0/\hbar\omega}{2\pi l^2}$ in our finite-range analysis [49]. Thus the interaction parameter in 2D is proportional to the factor λ_0 in front of the two-body potential [see Eq. (1)].

The Taylor expansion in (19) leads to two significant differences between the zero-range spectrum and the finite-range spectrum already presented in Fig. 2. First, when the interaction is repulsive, i.e., $\lambda_0 > 0$, Eq. (20) yields an additional deeply bound state which is not present in the original finite-range spectrum (see also [50] for the case of hard spheres in three dimensions, where also a redundant state appears in the zero-range pseudopotential approximation). This state appears due to the different asymptotic behavior of both sides of (19) in the limit $E/\hbar\omega \to -\infty$. While the LHS of (19) converges to 0, the expanded RHS diverges to $+\infty$; see Fig. 4. This also leads to a second difference. The finite-range result yields a bound state with an energy approaching $-\infty$ for $\lambda_0 \to -\infty$, while the zero-range equation yields a finite value which corresponds to the zero crossing appearing for negative $E/\hbar\omega$ in Fig. 2. This demonstrates that the short-range

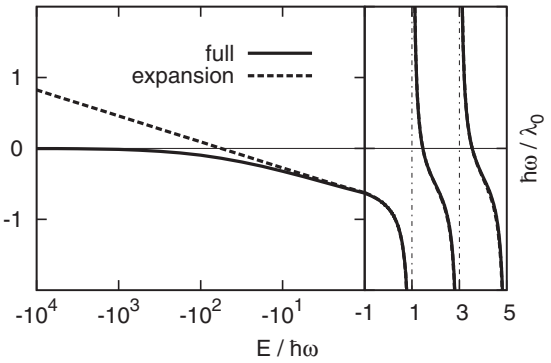

FIG. 4. Plot of the LHS (thick line) and the RHS (dashed line) of Eq. (19) versus $E/\hbar\omega$ for $l = 1$ and $s/l = 0.1$. For $E/\hbar\omega > -1$ the two curves are practically indistinguishable. The vertical dashed-dotted lines show the poles of both sides of Eq. (19). Notice the logarithmic scale on the x axis. See text for discussion. All quantities are dimensionless.

2D Gaussian-shaped interaction potential and the zero-range potential approximate each other well except for the ground state.

Equating the RHS of Eqs. (20) and (18) allows us to obtain a connection between the 2D scattering length, a_{2D}, and the parameters of the Gaussian-shaped potential λ_0 and s. Using $A = 2\ \ln(2) - 2\gamma$ from [26], and noticing that the authors use the definition of the harmonic-oscillator length with the full mass, we obtain

$$a_{2D} \approx \sqrt{2}s\, e^{-\frac{\gamma}{2} - \frac{\pi l^2}{\lambda_0 \hbar\omega}} \tag{21}$$

for the 2D scattering length of a Gaussian-shaped potential of width $s/l \ll 1$. We find good quantitative agreement when we compare the above expression for a_{2D} with numerical values from [31]. For $\sigma = 2^{-1/2}s = 0.1$ and $g = \lambda_0 = 1$, the relative difference between our analytical estimate and the numerical value is about 1%. Even in the regime of $\sigma = 2^{-1/2}s = 1$ and $g = \lambda_0 = 10$, where the accuracy of our treatment is limited, the relative difference is only about 8%.

VI. SUMMARY

We analyzed the problem of two harmonically trapped particles in 2D, which interact via a finite-range Gaussian-shaped two-body potential. We derived an approximative transcendental equation for the energy which is demonstrated to be highly accurate for the ground state. Moreover, our ansatz works well also for the excited states (see Appendix D). Using the Gaussian-shaped potential we were able to directly study the dependence of the ground-state energy on the range of the interaction. We recall that in the limit of zero-range interaction, it has been shown that the results are universal, i.e., the spectrum is independent of the details of short-range potential [26]. We found that the effect of the short-range interaction on the ground-state energy vanishes logarithmically with deceasing of the potential range, s, for all positive interaction strengths. This study is complemented by a variational treatment which shows that in the limit of a (nonregularized) δ potential, i.e., $s \to 0$, the energy spectrum of the two (repelling) particles can be made arbitrarily close to the respective noninteracting one by increasing the size of the Hilbert space. Furthermore, we demonstrated that an extremely large Hilbert space is required to approach the ground state when one is to tackle the limit of zero-range interaction numerically, providing thereby numerical incentive for using the Gaussian-shaped potential with a truly finite range as a model of the two-body interaction in many-particle simulations. Finally, we established and discussed the connection between our finite-range result and earlier zero-range treatments reported in the literature.

Our analysis shows that a Gaussian-shaped two-body potential and its zero-range pseudopotential give similar results for both repulsive and attractive interactions except for the lowest eigenstate of the latter potential. Here, for repulsion the zero-range pseudopotential leads to an additional dimer bound state which is not connected to the unperturbed system when the interaction is switched off. Consequently, this dimer state is difficult to reach when the interaction is smoothly switched on.

Going beyond two particles, as mentioned above, analytical treatments quickly become inaccessible, leaving one only with a numerical recourse. The results of the present work support the applicability of the Gaussian-shaped potential as a model of the two-body interaction in simulations of the statics (see [31]) and the nonequilibrium dynamics of trapped interacting bosons in 2D. Our experience in the nonequilibrium dynamics of interacting bosons in one dimension—computed by the multiconfigurational time-dependent Hartree [38–42,51,52] for bosons [53–59] methods—leaves nothing less than great expectations for the respective dynamics in 2D.

ACKNOWLEDGMENTS

We thank Kaspar Sakmann for very helpful discussions. Financial support by the Deutsche Forschungsgemeinschaft (DFG) also within the framework of the Enable fund of the excellence initiative at Heidelberg university is acknowledged.

APPENDIX A: EVALUATION OF THE MATRIX ELEMENTS

Here we outline the calculation of the matrix elements in Eq. (7) of the main text. The radial part of the zero angular momentum eigenfunctions of the 2D harmonic oscillator can be written in terms of the Laguerre polynomials $L_k(x)$. With $l = \sqrt{\frac{\hbar}{\mu\omega}}$ the eigenstates read [60]

$$\varphi_k(r) = \sqrt{2}l^{-1}e^{-\frac{r^2}{2l^2}} L_k\left(\frac{r^2}{l^2}\right). \tag{A1}$$

We need to evaluate the integral

$$I_{k',k} = 2l^{-2}\int_0^\infty e^{-\frac{r^2}{2l^2}} L_{k'}\left(\frac{r^2}{l^2}\right)\frac{e^{\frac{-r^2}{s^2}}}{\pi s^2} e^{-\frac{r^2}{2l^2}} L_k\left(\frac{r^2}{l^2}\right) r\, dr. \tag{A2}$$

We start by setting $\Lambda = 1 + \frac{l^2}{s^2}$ and rewriting

$$I_{k',k} = \frac{2l^{-2}}{\pi s^2} \int_0^\infty e^{-\Lambda \frac{r^2}{l^2}} L_{k'}\left(\frac{r^2}{l^2}\right) L_k\left(\frac{r^2}{l^2}\right) r\, dr. \quad \text{(A3)}$$

Now we define a new variable $\rho = \frac{\Lambda}{l^2} r^2$ and obtain

$$I_{k',k} = \frac{1}{\pi \Lambda s^2} \int_0^\infty e^{-\rho} L_{k'}(\Lambda^{-1}\rho) L_k(\Lambda^{-1}\rho) d\rho. \quad \text{(A4)}$$

To get rid of the Λ^{-1} factor in the argument of $L(\Lambda^{-1}\rho)$ we use the known multiplication formula for Laguerre polynomials [43],

$$L_k(\Lambda x) = \sum_{i=0}^{k} \binom{k}{i} \Lambda^i (1-\Lambda)^{k-i} L_i(x). \quad \text{(A5)}$$

By substituting the above expression for $L_k(\Lambda^{-1}\rho)$ and $L_{k'}(\Lambda^{-1}\rho)$ into the integral of Eq. (A4), and by making use of the orthogonality of the Laguerre polynomials with respect to the weight function $e^{-\rho}$, we obtain

$$I_{k',k} = \frac{1}{\pi \Lambda s^2} \sum_{i=0}^{\min\{k,k'\}} \binom{k}{i} \binom{k'}{i} \Lambda^{-2i} (1-\Lambda^{-1})^{k+k'-2i}. \quad \text{(A6)}$$

We can write the above expression as

$$I_{k',k} = \frac{1}{\pi \Lambda s^2} \left(\frac{\Lambda - 1}{\Lambda}\right)^{k+k'} \sum_{i=0}^{\min\{k,k'\}} \binom{k}{i} \binom{k'}{i} \left(\frac{1}{(\Lambda-1)^2}\right)^i. \quad \text{(A7)}$$

In order to express the sum in terms of the Gauss hypergeometric function ${}_2F_1(a,b;c,z)$, we rewrite the above expression using the Pochhammer symbols $(x)_i$ for the rising factorial [43],

$$I_{k',k} = \frac{1}{\pi \Lambda s^2} \left(\frac{\Lambda - 1}{\Lambda}\right)^{k+k'} \sum_{i=0}^{\min\{k,k'\}} \frac{(-k)_i (-k')_i}{(1)_i} \frac{\left(\frac{1}{(\Lambda-1)^2}\right)^i}{i!}. \quad \text{(A8)}$$

We can now directly use the definition of ${}_2F_1(a,b;c,z)$ [43] and obtain

$$I_{k',k} = \frac{1}{\pi \gamma s^2} \left(\frac{\Lambda - 1}{\Lambda}\right)^{k+k'} {}_2F_1\left(-k', -k; 1, \left(\frac{1}{\Lambda - 1}\right)^2\right). \quad \text{(A9)}$$

Finally, by changing back to the original variables, we arrive at Eq. (7) of the main text.

APPENDIX B: VARIATIONAL ENERGY

Here we show that the approach in Sec. III for the energy spectrum of the nonregularized δ potential is essentially a variational treatment with $\Psi = \sum_{i=0}^{N} c_k \varphi_k$ and $c_k = \frac{\text{const}}{\varepsilon_k - E}$. For this purpose, let us consider E just as a parameter which fulfills Eq. (11) for a given λ_0 and fixed finite N. The variational energy then reads

$$\begin{aligned}\langle \Psi | H_{\text{rel}} | \Psi \rangle &= \int d\bar{r} \left(\sum_{k=0}^{N} c_k \varphi_k^*\right) H_{\text{rel}} \left(\sum_{k'=0}^{N} c_{k'} \varphi_{k'}\right) \\ &= \sum_{k=0}^{N} \frac{\text{const}^2}{\varepsilon_k - E} \left[\frac{\varepsilon_k}{\varepsilon_k - E} + \frac{\lambda_0}{\pi l^2} \sum_{k'=0}^{N} \frac{1}{\varepsilon_{k'} - E}\right] \\ &= \sum_{k=0}^{N} \frac{\text{const}^2}{\varepsilon_k - E} \left[\frac{\varepsilon_k}{\varepsilon_k - E} - 1\right] \\ &= \sum_{k=0}^{N} E \frac{\text{const}^2}{(\varepsilon_k - E)^2} = E. \end{aligned} \quad \text{(B1)}$$

We thus see that the variational energy is indeed equal to E. In the last step we used the normalization condition for the wave function $\sum_{k=0}^{N} |c_k|^2 = 1$.

APPENDIX C: ANSATZ FOR c_k IN THE FINITE-RANGE CASE

Here we discuss the ansatz for the expansion coefficients in Eq. (13). We stress that the approach is general. Let us consider a Hamilton operator

$$H = H_0 + \lambda_0 W \quad \text{(C1)}$$

and assume that the eigenstates and eigenenergies of H_0 are known. We denote them by $|\phi_k\rangle$ with $H_0|\phi_k\rangle = \varepsilon_k |\phi_k\rangle$. For an eigenstate $|\Psi\rangle = \sum c_k |\phi_k\rangle$ of the full Hamilton operator H we can write

$$(H_0 + \lambda_0 W)|\Psi\rangle = E|\Psi\rangle,$$

or, equivalently,

$$(E - H_0)|\Psi\rangle = \lambda_0 W|\Psi\rangle. \quad \text{(C2)}$$

After projection on an unperturbed state $\langle\phi_k|$, we express the above equation in the form

$$(E - \varepsilon_k)\langle\phi_k|\Psi\rangle = \lambda_0 \langle\phi_k|W|\Psi\rangle. \quad \text{(C3)}$$

From here we obtain a symbolic expression for the expansion coefficients

$$c_k = \langle\phi_k|\Psi\rangle = \frac{\lambda_0 \langle\phi_k|W|\Psi\rangle}{(E - \varepsilon_k)} = -\frac{\lambda_0 \langle\phi_k|W|\Psi\rangle}{(\varepsilon_k - E)}. \quad \text{(C4)}$$

Until now we have not used any approximations. Of course, the above expression is only an implicit one, because the unknown state $|\Psi\rangle$, which is itself dependent on c_k, appears on the RHS. Our ansatz in Eq. (13) of the main text consists in taking only a "first-order approximation" for the expansion coefficients, i.e., we substitute $|\Psi\rangle = |\phi_0\rangle$ in (C4) and obtain

$$c_k = -\frac{\lambda_0 \langle\phi_k|W|\phi_0\rangle}{(\varepsilon_k - E)}. \quad \text{(C5)}$$

Of course, we can also substitute $|\Psi\rangle = |\phi_{k'}\rangle$, $k' \neq 0$ into Eq. (C5) and obtain similar expressions which might be more efficient when studying excited states.

TABLE I. Numerical values of $\frac{E_{DD}-E}{E_{DD}}$ for the ground state and several excited states with $\lambda_0 = 1.0$ and four different choices of s and $l = 1$. E_{DD} is the value obtained by direct diagonalization of the Hamiltonian and E is computed using Eq. (17).

	$s = 0.1$	$s = 0.2$	$s = 0.4$	$s = 0.5$
GS	6.1×10^{-4}	7.4×10^{-4}	6.9×10^{-4}	5.8×10^{-4}
1st	2.1×10^{-4}	9.2×10^{-5}	4.9×10^{-4}	1.7×10^{-3}
2nd	1.1×10^{-4}	1.6×10^{-5}	1.8×10^{-3}	4.1×10^{-3}
4th	3.4×10^{-5}	1.5×10^{-4}	3.5×10^{-3}	5.2×10^{-3}
8th	4.7×10^{-6}	5.7×10^{-4}	3.3×10^{-3}	3.4×10^{-3}
16th	3.9×10^{-5}	1.0×10^{-3}	1.7×10^{-3}	1.4×10^{-3}

APPENDIX D: NUMERICAL COMPARISON

In this section we compare energies obtained by solving Eq. (17) with the numerical values determined by the full direct diagonalization of the Hamiltonian using the matrix elements in Eq. (7). In Table I we show the relative difference between both values, i.e., $\frac{E_{DD}-E}{E_{DD}}$, where E_{DD} denotes the value obtained from direct diagonalization and E denotes the energy obtained by solving Eq. (17). The comparison is performed for the ground state (GS) and several excited states with zero angular momentum (see the first column in Table I). We observe an excellent agreement between the values from both methods, with $\frac{E_{DD}-E}{E_{DD}}$ in the order of 10^{-3} and below; see Table I.

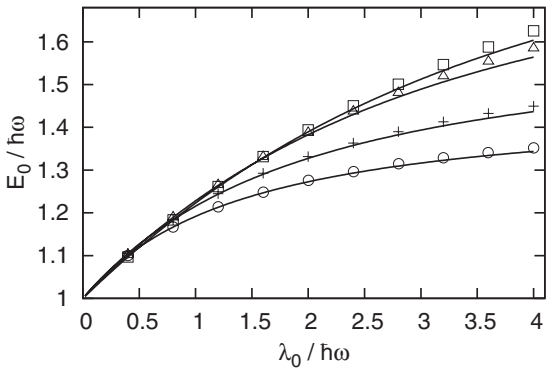

FIG. 5. Comparison between the ground-state energy E_0 versus λ_0 obtained from Eq. (17) (lines) and that computed by direct diagonalization (symbols). The widths from top to bottom are $s = 0.5$ (squares), 0.4 (triangles), 0.2 (crosses), 0.1 (circles), and $l = 1$. See text for more details. All quantities are dimensionless

Finally, we perform a study of the ground-state energy for different widths, $s = 0.1$, 0.2, 0.4, and 0.5, as a function of λ_0. The results are shown in Fig. 5, where we plot the values of the ground-state energy as obtained from Eq. (17) and direct diagonalization. The values obtained from Eq. (17) are in a very good agreement with the ones from direct diagonalization for $\lambda_0/\hbar\omega$ up to 4. Analogous behavior was also found for the excited states.

[1] D. J. Bishop and J. D. Reppy, Phys. Rev. Lett. **40**, 1727 (1978).
[2] P. Minnhagen, Rev. Mod. Phys. **59**, 1001 (1987).
[3] M.-C. Cha, M. P. A. Fisher, S. M. Girvin, M. Wallin, and A. P. Young, Phys. Rev. B **44**, 6883 (1991).
[4] G. T. Seidler, T. F. Rosenbaum, and B. W. Veal, Phys. Rev. B **45**, 10162 (1992).
[5] N. Marković, C. Christiansen, A. M. Mack, W. H. Huber, and A. M. Goldman, Phys. Rev. B **60**, 4320 (1999).
[6] K. S. Novoselov, Rev. Mod. Phys. **83**, 837 (2011).
[7] S. Das Sarma, S. Adam, E. H. Hwang, and E. Rossi, Rev. Mod. Phys. **83**, 407 (2011).
[8] B. Partoens, A. Matulis, and F. M. Peeters, Phys. Rev. B **59**, 1617 (1999).
[9] D. S. Petrov, D. M. Gangardt, and G. V. Shlyapnikov, J. Phys. IV **116**, 5 (2004).
[10] A. Görlitz, J. M. Vogels, A. E. Leanhardt, C. Raman, T. L. Gustavson, J. R. Abo-Shaeer, A. P. Chikkatur, S. Gupta, S. Inouye, T. Rosenband, and W. Ketterle, Phys. Rev. Lett. **87**, 130402 (2001).
[11] S. Burger, F. S. Cataliotti, C. Fort, P. Maddaloni, F. Minardi, and M. Inguscio, Europhys. Lett. **57**, 1 (2002).
[12] D. Rychtarik, B. Engeser, H.-C. Nägerl, and R. Grimm, Phys. Rev. Lett. **92**, 173003 (2004).
[13] Z. Hadzibabic, S. Stock, B. Battelier, V. Bretin, and J. Dalibard, Phys. Rev. Lett. **93**, 180403 (2004).
[14] N. L. Smith, W. H. Heathcote, G. Hechenblaikner, E. Nugent, and C. J. Foot, J. Phys. B **38**, 223 (2005).
[15] K. Martiyanov, V. Makhalov, and A. Turlapov, Phys. Rev. Lett. **105**, 030404 (2010).
[16] R. Jackiw, *Diverse Topics in Theoretical and Mathematical Physics* (World Scientific, Singapore, 1995).
[17] T. Busch, B.-G. Englert, K. Rzążewski, and M. Wilkens, Found. Phys. **28**, 549 (1998).
[18] L. R. Mead and J. Godines, Am. J. Phys. **59**, 935 (1991).
[19] R. M. Cavalcanti, Rev. Bras. Ensino Fis. **21**, 336 (1999).
[20] S.-L. Neyo, Am. J. Phys. **68**, 571 (1999).
[21] A. Sütő, J. Stat. Phys. **109**, 1051 (2002).
[22] B. D. Esry and C. H. Greene, Phys. Rev. A **60**, 1451 (1999).
[23] V. S. Araujo, F. A. B. Coutinho, and J. F. Perez, Am. J. Phys. **72**, 203 (2004).
[24] S. Albeverio, F. Gesztesy, R. Hoegn-Krohn, and H. Holden, *Solvable Models in Quantum Mechanics* (AMS Chelsea, Providence, 2004).
[25] K. Wódkiewicz, Phys. Rev. A **43**, 68 (1991).
[26] A. Farrell and B. P. van Zyl, J. Phys. A **43**, 015302 (2010).
[27] T. K. Lim and P. A. Maurone, Phys. Rev. B **22**, 1467 (1980).
[28] X.-J. Liu, H. Hu, and P. D. Drummond, Phys. Rev. B **82**, 054524 (2010).
[29] K. Kanjilal and D. Blume, Phys. Rev. A **73**, 060701(R) (2006).
[30] N. T. Zinner, J. Phys. A **45**, 205302 (2012).
[31] J. Christensson, C. Forssén, S. Åberg, and S. M. Reimann, Phys. Rev. A **79**, 012707 (2009).
[32] A. Posazhennikova, Rev. Mod. Phys. **78**, 1111 (2006).

[33] I. Bloch, J. Dalibard, and W. Zwerger, Rev. Mod. Phys. **80**, 885 (2008).
[34] S. Zöllner, H.-D. Meyer, and P. Schmelcher, Phys. Rev. A **74**, 053612 (2006).
[35] S. Zöllner, H.-D. Meyer, and P. Schmelcher, Phys. Rev. A **74**, 063611 (2006).
[36] S. Zöllner, H.-D. Meyer, and P. Schmelcher, Phys. Rev. A **75**, 043608 (2007).
[37] I. Brouzos, S. Zöllner, and P. Schmelcher, Phys. Rev. A **81**, 053613 (2010).
[38] C. Matthies, S. Zöllner, H.-D. Meyer, and P. Schmelcher, Phys. Rev. A **76**, 023602 (2007).
[39] S. Zöllner, H.-D. Meyer, and P. Schmelcher, Phys. Rev. Lett. **100**, 040401 (2008).
[40] S. Zöllner, H.-D. Meyer, and P. Schmelcher, Phys. Rev. A **78**, 013621 (2008).
[41] B. Chatterjee, I. Brouzos, S. Zöllner, and P. Schmelcher, Phys. Rev. A **82**, 043619 (2010).
[42] I. Brouzos and P. Schmelcher, Phys. Rev. A **85**, 033635 (2012).
[43] *Handbook of Mathematical Functions*, edited by M. Abramowitz and A. Stegun (Dover, New York, 1972).
[44] M. L. Boas, *Mathematical Methods in the Physical Sciences* (John Wiley and Sons, New York, 1983).
[45] W. Magnus, F. Oberhettinger, and F. G. Tricomy, *Higher Transcendental Functions* (McGraw-Hill, New York, 1953).
[46] C. N. Friedman, J. Funct. Anal. **10**, 346 (1972).
[47] H. Lee, H. Hsu, and L. E. Reichl, Phys. Rev. B **71**, 045307 (2005).
[48] S. Wolfram, *Mathematica 8* (Wolfram Research Inc., Champaign, IL, 2011).
[49] We can also obtain this directly by substituting (21) in $\ln(\frac{l^2}{2a_{2D}^2})^{-1}$ and expanding for small λ_0, which leads to $\ln(\frac{l^2}{2a_{2D}^2})^{-1} \approx \frac{\lambda_0/\hbar\omega}{2\pi l^2}$.
[50] M. Block and M. Holthaus, Phys. Rev. A **65**, 052102 (2002).
[51] H.-D. Meyer, U. Manthe, and L. Cederbaum, Chem. Phys. Lett. **165**, 73 (1990).
[52] U. Manthe, H.-D. Meyer, and L. S. Cederbaum, J. Chem. Phys. **97**, 3199 (1992).
[53] A. I. Streltsov, O. E. Alon, and L. S. Cederbaum, Phys. Rev. Lett. **99**, 030402 (2007).
[54] O. E. Alon, A. I. Streltsov, and L. S. Cederbaum, Phys. Rev. A **77**, 033613 (2008).
[55] A. I. Streltsov, O. E. Alon, and L. S. Cederbaum, Phys. Rev. Lett. **100**, 130401 (2008).
[56] K. Sakmann, A. I. Streltsov, O. E. Alon, and L. S. Cederbaum, Phys. Rev. Lett. **103**, 220601 (2009).
[57] A. I. Streltsov, O. E. Alon, and L. S. Cederbaum, Phys. Rev. Lett. **106**, 240401 (2011).
[58] A. U. J. Lode, A. I. Streltsov, K. Sakmann, O. E. Alon, and L. S. Cederbaum, Proc. Natl. Acad. Sci. USA **109**, 13521 (2012).
[59] A. U. J. Lode, K. Sakmann, O. E. Alon, L. S. Cederbaum, and A. I. Streltsov, Phys. Rev. A **86**, 063606 (2012).
[60] S. Flügge, *Practical Quantum Mechanics I* (Springer, Berlin, 1971), Vol. 1.